



CONTROL OF A SYSTEM OF ENERGY BASED ON FLYWHEEL TO MITIGATE THE VOLTAGE GAPS AT THE POINT OF COMMON COUPLING

CONTROL DE UN SISTEMA DE ENERGÍA BASADO EN VOLANTES DE INERCIA PARA MITIGAR LOS HUECOS DE TENSION EN EL PUNTO DE CONEXIÓN COMÚN

Carlos Orellana Uguña^{1,*}, Luis González Morales², Nuno Abreu Sousa³

Abstract

This article presents the design of a power system based on flywheel to mitigate voltage sags. With this system the power quality is improved at a point in a distribution network, which is subject to the random connection of electric machines. For this purpose, the power distribution system is modeled, the power supply system which is composed of an electric machine with flywheel, the bidirectional energy conversion system and the current, voltage and speed control system. The designed system enables supplying a power of 22.8 kW and capacity of 1.2 Wh, compensating the transients produced by the loads connected to the network.

Keywords: Batteries, flywheel, AC/DC, DC/AC, PCC.

Resumen

Este artículo presenta el diseño de un sistema de energía basado en volante de inercia para mitigar los huecos de tensión. Con el sistema se mejora la calidad de energía en un punto de una red de distribución, el cual está expuesto a la conexión aleatoria de máquinas eléctricas. Para ello, se modela el sistema de distribución de energía, el sistema de inyección de energía que está compuesto por una máquina eléctrica con volante de inercia, el sistema de conversión de energía bidireccional y el sistema de control de corriente, voltaje y velocidad. El sistema diseñado permite inyectar una potencia de 22.8 kW y capacidad de 1.2 Wh, compensando los transitorios producidos por las cargas conectadas a la red.

Palabras clave: baterías, volante de inercia, AC/DC, DC/AC, PCC.

^{1,*}Instituto Tecnológico Superior Luis Rogerio González, Azogues – Ecuador.

Corresponding author✉: carl.mauryou@yahoo.es. <http://orcid.org/0000-0001-7214-4060>

²Departamento de Ingeniería Eléctrica Electrónica y Telecomunicaciones (DEET), Universidad de Cuenca, Cuenca – Ecuador. <http://orcid.org/0000-0001-9992-3494>

³Departamento de Engenharia Electrotécnica da Escola Superior de Tecnologia e Gestão Instituto Politécnico de Leiria - Portugal. <http://orcid.org/0000-0002-3837-0547>

Received: 22-01-2020, accepted after review: 19-05-2020

Suggested citation: Orellana Uguña, C.; González Morales, L. and Abreu Sousa, N. (2020). «Control of a System of Energy based on Flywheel to mitigate the Voltage Gaps at the Point of Common Coupling». *INGENIUS*. N.º 24, (july-december). pp. 49-58. DOI: <https://doi.org/10.17163/ings.n24.2020.05>.

1. Introduction

Since the electric power distribution company is responsible for supplying power to the consumers based on established standards, it is under the obligation to maintain the quality of the delivered power, and such quality can be estimated by means of the service continuity and the quality of the voltage waveform.

In order to carry out this objective, different power backup strategies were implemented in electrical power systems, which seek to improve the power quality and stability [1]. According to their discharge time [2], these systems may be classified as follows:

Discharge time from seconds to minutes: are used to improve the power quality. The discharge times are of 10 minutes with responses in milliseconds. This type of systems include the supercapacitors with powers up to 1 MW, and the flywheels with powers between 10 kW and 1 MW.

Discharge time from minutes to one hour: are used as power bridges, i.e., they ensure the reliability of the supply source to the users, have responses from seconds to minutes with discharge times of up to 1 hour, and powers between 1 kW and 10 MW. Electrochemical batteries are included in this type.

Discharge time in hours: they are utilized for energy management; this type includes the pumped and compressed air hydraulic energy storage, with powers between 100 MW and 1 GW, respectively, and the thermal energy storage with storage capacities between 10 MW and 100 MW.

Regardless of the technology used, it must be considered aspects such as: operating and constructive expenditures, life cycle, response time after the occurrence of a disturbance in the network, geographical limitations and physical properties [3].

If geographical limitations are considered, the pumped storage systems are ruled out, since they require two reservoirs located at different levels because the energy stored is proportional to the volume of liquid and to the difference between the heights of the reservoirs, thus its installation is limited to places with non-planar characteristics.

Compressed air is neither chosen because it requires very resistant underground caverns to house air at high pressure and, at last, the thermal energy storage is discarded since the operating principle of each of them depends on the working ambient temperature.

As a result, electrochemical batteries, flywheels and supercapacitors are the options remaining [2].

The electrochemical batteries exhibit drawbacks, such as: at the end of their useful life they pollute the environment because an adequate recycling infrastructure is not available [4], their useful life depends

on the working environment and on the number of charges/discharges and, the most important, they cannot be charged nor discharged quickly because they have a large internal resistance [5].

Therefore, the use of the flywheels is the option remaining, which offer the following advantages: a greater cycle of charges/discharges with medium to high power (kW to MW) during short periods of time (seconds) without affecting their useful life [6], high response capacity, friendly to the environment since they do not require chemical reactions, and no special geographical conditions are needed for their construction [7].

In comparative terms, the main competitors of the flywheels are the supercapacitors, which similarly offer the following advantages over electrochemical batteries: they may be charged/discharged in short periods of time (seconds), may supply high charge currents, have a life cycle of the order of millions of times, operate under very tough temperature conditions, and do not have toxic elements in their structure [2].

In this work it is intended to carry out the study about the design of a power supply system based on flywheels, to mitigate the voltage sags in the common connection point of an electrical distribution system. For this purpose, it will be modeled the flywheel with its control system and the distribution network. The design is applied to a rural area with mining and agricultural activities with electric machines as loads, using PSIM® as simulation tool.

1.1. Problem description

Due to the increase in the loads connected to the common connection point (CCP) belonging to the mining and agricultural area under study, the power supply quality decreases, due to the features of the existing distribution system and the continuous start-up of high-capacity electric machines, and also soft starters that contribute to the occurrence of voltage sags.

The case study will cover the Pucará canton and surroundings, specifically the San Juan de Naranjillas village belonging to the Azuay province, Ecuador, which is supplied by the feeder 1424 of the South Regional Electric Company (Empresa Eléctrica Regional Sur).

Due to the lack of technical standards that regulate the power of the motors utilized in the different mining/agricultural activities, it was considered as reference the machinery utilized in a main mining company called TRES CHORRERAS, which establishes the use of 32 HP Allis Chalmers motors, and according to this and catalogs available in Ecuador, W21 50 HP Explosion-proof NEMA Premium electric motors are utilized to drive centrifugal pumps for liquid handling, crushers, conveyor belts, among others [8].

The features of the motors to be utilized are indicated in Figure 1 [9].

The simulation model of the distribution network is indicated in Figure 1, with resistances of 20Ω that emulate small electrical equipment distributed in each of the phases (lightning, appliances).

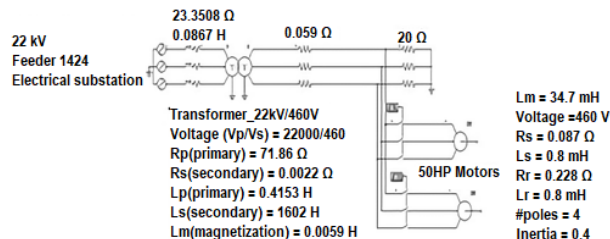


Figure 1. Model of the distribution network and features of the 50 HP motors.

1.2. Power quality

One of the important aspects related to the power quality are the so-called voltage sags, described in detail in the technical standards IEEE 1159, CONELEC 004/01 and NP EN 50160-2010, which define them as a decrease in the supply voltage to a value between 10 % and 90 % of the nominal voltage.

In addition, the standards define the voltage swell as an increase in the supply voltage to a value between 110 % and 180 % of the nominal voltage, followed by a voltage restore after a short period of time. Applying this criterion to the phase-to-neutral voltage level of the secondary side of the transformer of Figure 1, the range for the occurrence of sags is between 26.55 V and 238.95 V, and for swells between 292.05 V and 477.9 V, thus resulting in a permissible range from 238.95 V to 292.05 V.

The methods utilized in this work to mitigate the occurrence of voltage sags are described in the following.

2. Materials and Methods

2.1. Proposed power system for the mitigation of voltage sags in the common connection point

Figure 2 shows the block diagram model proposed by this study to mitigate the voltage sags in the CCP, which is constituted by an electrical machine with flywheel, two controlled three-phase power converters and a coupling capacitor called DC-link.

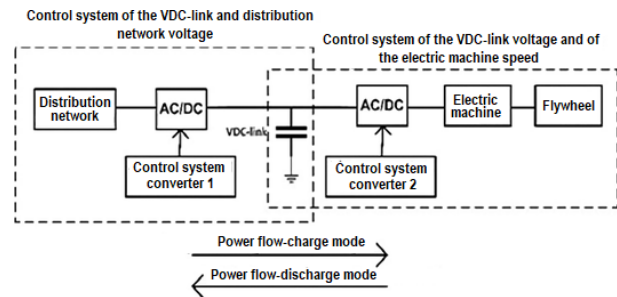


Figure 2. System based on flywheel to mitigate voltage sags in the CCP.

In Figure 2, the proposed model consists of the followings control stages:

Control system 1: The power converter associated to the distribution network consists of a control of current in the synchronous reference system such as the utilized in [10,11]. Its task is to control the distribution network voltage and the DC-link voltage. This control may be divided in two sub-stages: charge mode, power flows from the distribution network to the direct current bus to reach the nominal value of $V_{DC-link}$. In this mode, the $V_{DC-link}$ control system operates using the converter as a controlled three-phase rectifier. In discharge mode, power flows from the direct current bus to the distribution network, in this mode, the control system of the distribution network voltage operates using the converter as a controlled three-phase inverter.

Control system 2: the power converter associated to the electric machine consists of a control of current in the synchronous reference system. This control system can be divided in two sub-stages: charge mode, power flows from the $V_{DC-link}$ voltage source to the electric machine that is operating as a motor to reach the nominal speed of charge, in this mode, the electric machine speed control system operates using the converter as a controlled three-phase inverter. In this state, the energy of the system is stored as kinetic energy. In discharge mode, power flows from the electric machine operating as a generator to the $V_{DC-link}$ source, to maintain the voltage at a reference value in the presence of any load connected to the distribution network. In this mode, the control system of the voltage $V_{DC-link}$ of the intermediate circuit operates using the converter as a controlled three-phase rectifier.

The change between the control modes is subject to the voltage at the CCP; in this sense, each of the power converters will operate as AC/DC or DC/AC.

The control loops that constitute the power supply system based on flywheel are described in the following.

2.1.1. Control system 1, belonging to the control of the distribution network voltage and of the $V_{DC-link}$ voltage.

The control system 1 has a structure defined by the charge or discharge operation mode. Figure 3 shows a block diagram of the cascade control system.

Due to the voltage level which are able to withstand the SKiM459GD12E4 three-phase converter and the coupling capacitor U37F type E37F501CPN103MFK0M, a voltage level of 900 Vdc was established as reference for the $V_{DC-link}$.

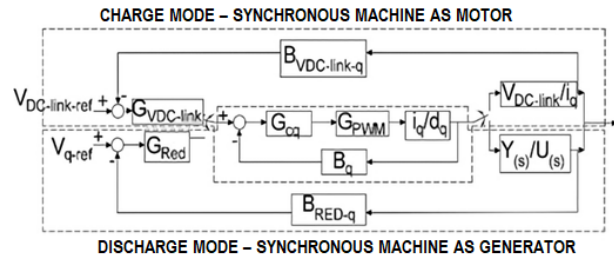


Figure 3. Control loops of the distribution network voltage and of the $V_{DC-link}$ voltage.

From Figure 3, B_q , B_{Red-q} , $B_{VDC-link}$ are the gains associated to the measurements of current, distribution network voltage and $V_{DC-link}$ voltage, respectively, with unit values, G_{cq} , $G_{VDC-link}$, $G_{network}$ are the transfer functions of the controllers, where in this application classical controllers of proportional-integral (PI) configuration are utilized, G_{PWM} is the gain of the PWM, a unit gain has been used in this case, $\frac{Y(s)}{U(s)}$ represents the transfer function that relates the distribution network voltage with respect to the current in the quadrature axis, and $\frac{V_{DC-link}}{\tilde{i}_q}$ is the transfer function that relates the $V_{DC-link}$ voltage with respect to the current in the quadrature axis.

The power converter can be modeled through equation 1, as utilized in [10, 11].

$$\frac{\tilde{i}'_d(s)}{\tilde{d}'_d(s)} = \frac{\tilde{i}'_q(s)}{\tilde{d}'_q(s)} = \frac{V_0}{Ls' + R_s} \quad (1)$$

The following is considered regarding the parameters involved in Equation 1:

V_0 is the $V_{DC-link}$ voltage, which in the present work has been defined at a value of 900 V.

According to [12], L is the inductance of the input filter. For the calculation it is proceeded in the following way: the inductive reactance

is considered equal to 10 % of the base resistance [10], thus resulting $Xl = 0,565 \Omega$, and therefore, $L = 1,5 mH$. From this initial value L is calibrated until reaching a value of $7 mH$, with which the total harmonic distortion (THD) fulfills the standard NP EN 50160-2010, Conelec 004/01 (smaller than 8 %).

According to [12], R_s is associated to the losses of the passive elements and semiconductors in the converter.

s' is the Laplace operator.

Similarly, the energy balance equations associated to the capacitor of the bus, which can be represented by means of equations (2) and (3) [10], are also honored.

$$\frac{V_{DC-link}}{\tilde{i}_q} = \frac{D_q}{Cs' + \frac{I_0}{V_{DC-link}}} \quad (2)$$

$$D_q = \frac{2\sqrt{2}V_{f-n}}{V_{DC-link}} \quad (3)$$

Where: D_q is the modulation index, C is the total capacitance of the capacitors that constitute the direct current bus, I_0 is the current that circulates from the rectifier bridge to the direct current bus, $V_{DC-link}$ is the voltage of the direct current bus, s' is the Laplace operator.

In the case of the discharge mode, the power converter controlled by means of the current loops in the direct and quadrature axes is utilized for controlling the voltage in the distribution network by means of the transfer function $\left(\frac{Y(s)}{U(s)}\right)$, which for the design of the control system has been characterized as a first order approximation. In order to find the parameters that constitute such transfer function, it is considered that the system based on the flywheel will be connected in parallel to the distribution network behaving as a current source. Graphically, Figure 4 shows the scheme to determine the previously described transfer function by means of the step response.

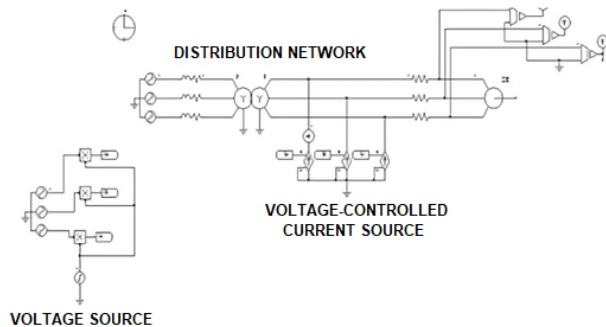


Figure 4. Model for the transfer function that relates the voltage at the CCP with the supply of current in phase.

When applying the previously described procedure, the behavior of the distribution network voltage after a disturbance in current with amplitude $\Delta I = 400$ A results in $\Delta V = 51,6$ V, obtaining a transfer function as the one given by Equation 4.

$$\frac{Y(s)}{U(s)} = \frac{0,129}{0,287s' + 1} \quad (4)$$

It is important to remark that the currents supplied from the energy storage system to the CCP, require a phase synchronization system to control the active or reactive power. A normalized phase-locked loop (PLL) system as the one used in [10] has been utilized in this design.

2.1.2. Control system 2, belonging to the control of the electric machine speed and of the $V_{DC-link}$ voltage.

The electric machine used in the present work is a permanent magnet synchronous machine, since it presents advantages over the induction machines, such as: high efficiency, excellent power density, good mechanical torque/current ratio and small size [13]. It should be remarked that in synchronous machines the speed of the rotor is equal to the speed of the rotor flux. Therefore, θ_1 (angle necessary for the Park transformation) is directly measured by means of position sensors or by means of the integration of the rotor speed [14].

A field-oriented control (FOC) was utilized to control de synchronous machine speed, which enables decoupling the mechanical torque and the components of the magnetization flux, due to simplicity of being able to independently control the currents i_{sd} (associated to the magnetic flux of the machine) and i_{sq} (associated to the mechanical torque exerted by the machine), thanks to its smooth rotor ($L_d = L_q$) [10].

The mathematical model of the permanent magnet synchronous machine in the synchronous reference system is expressed by Equations 5 and 6.

$$V_d = R_s I_d - w L_q I_q + L_d \frac{dI_d}{dt} \quad (5)$$

$$V_q w L_d I_d + R_s I_q + L_q \frac{dI_q}{dt} + \lambda_m \frac{\sqrt{6}}{2} w \quad (6)$$

Where: w is the electric angular speed in (rad/s); λ_m is the flux of the permanent magnets, L_q and L_d are the inductances of the machine in the quadrature and direct synchronous axes, respectively, in (H); R_s is the resistance of the stator of the synchronous machine in (Ω).

The effective power and the torque are expressed by Equations 7 and 8.

$$P_e = w \left[(L_d - L_q) I_q I_d + \lambda_m I_q \frac{\sqrt{6}}{2} \right] \quad (7)$$

$$T_e = p \left[(L_d - L_q) I_q I_d + \lambda_m I_q \frac{\sqrt{6}}{2} \right] \quad (8)$$

Where: p is the number of poles of the synchronous machine.

The relationship between the angular speed of the rotor and the current referred to the quadrature axis, is expressed by Equation 9.

$$\frac{dw_r}{dt} + B w_r = p \lambda_m I_q \frac{\sqrt{6}}{2} \quad (9)$$

Where: J is the moment of inertia in ($kg \cdot m^2$), B is the friction coefficient in ($N \cdot m \cdot s$) and w_r is the mechanical angular speed.

The relationship between the steady-state current in the quadrature axis and the voltage of the capacitor of the direct-current bus is expressed by means of Equation 10.

$$I_{qs} = \frac{V_{DC-link} I_{dc}}{p \lambda_m \frac{\sqrt{6}}{2} w_r} \quad (10)$$

From the equations of the synchronous machine together with the capacitor referred to the synchronous axis, it is obtained the block diagram shown in Figure 5, where it is observed an internal loop belonging to the current loop in the quadrature axis and two external loops that correspond to the control of the synchronous machine speed and the control of the $V_{DC-link}$ voltage [15].

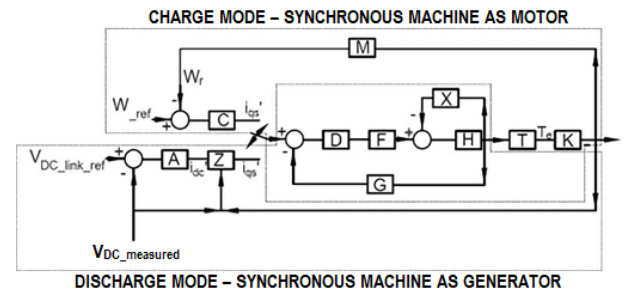


Figure 5. Control loop of the $V_{DC-link}$ voltage and of the synchronous machine speed.

From Figure 5, G and M are the gains associated to the measured values of current and speed, with unit values, and D, A, C are the transfer functions of the controllers. PI controllers have been used in this application; F is the gain of the PWM, which in this case is a unit gain. H is expressed by equation (1), $Z = \frac{2V_{DC_medio} I_{dc}}{p \lambda_m \sqrt{6} w_r}$, $T = \frac{p \lambda_m \sqrt{6}}{2}$, $X = \left(\frac{p \lambda_m \sqrt{6}}{2} \right)^2 \left(\frac{1}{J s' + B} \right)$, $K = \frac{1}{J s' + B}$.

For tuning the speed and current loop, it is necessary to know the electric and mechanical parameters of the three-phase synchronous machine; these data are shown in Table 1 [15].

Table 1. Parameters of the permanent magnet synchronous machine

Power (kW)	< 125
Poles	2
Speed (krpm/min)	< 36
Resistance of the stator (Ω)	0,02
Inductance of the stator (μH)	entre 70 y 120
Inertia ($kg \cdot m^2$)	0,633
Coefficient of friction ($N \cdot m \cdot s$)	$4,2 \times 10^{-05}$
External inductance (mH)	1,5

The transfer function required for tuning the PI controller related to the control of the $V_{DC-link}$ voltage is the same given by equations 2 and 3.

Equations 11 and 12 are the result of the simplification of the loops of current and synchronous machine speed.

$$\frac{i_{qs}}{i'_{qs}} = \frac{Es'^2 + Ps' + N}{Qs'^3 + Is'^2 + Ys' + U} \quad (11)$$

Where:

$$E = 4JLV_{DC-link}, \quad P = (4LBV_{DC-link} + 4JRV_{DC-link}).$$

$$N = 4RB, \quad L = L_{synchronous-machine} + L_{external} \text{ belonging to the numerator of equation (11).}$$

$$Q = 4JL^2, \quad I = 4L^2B + 8JRL, \quad Y = 8RBL + 6V_{DC-link}p^2\lambda_m^2L, \quad U = 4R^2B + 6V_{DC-link}p^2\lambda_m^2R, \\ L = L_{synchronous-machine} + L_{external} \text{ belonging to the denominator of equation (11).}$$

$$\frac{w_r}{i_{qs}} = \frac{1,22p\lambda_m}{Js' + B} \quad (12)$$

The tuning of the PI controllers for the different control loops is carried out by assignment of poles and zeroes, considering the following aspects [11]:

In this work the switching frequency is set at 15 kHz, which limits the dynamics of the current loops, since for frequencies above $\frac{f_{sw}}{2} = 7.5 \text{ kHz}$, the modeling technique loses its validity.

From the tuning frequency of the PI for the current loop, it should be tuned a decade below for the remaining control loops.

The phase margin of the Bode plot has to be greater or equal to 60° electrical.

The gain margin is greater than or equal to 7 dB.

Considering these aspects, the following parameters of the PI controllers were obtained:

Control system 1: for the control loop of the direct and quadrature currents, the PI controller has $k_p = 0.36$ and $k_i = 0.09$, for the control loop of the direct current bus $V_{DC-link}$ voltage, the PI controller has $k_p = 51.02$ and $k_i = 0.32$, and for the control loop of the distribution network voltage, the PI controller has $k_p = 36.98$ and $k_i = 4.3$.

Control system 2: for the control loop of the direct and quadrature currents, the PI controller has $k_p = 655$ and $k_i = 166.62$, for the control loop of the $V_{DC-link}$ voltage of the direct current bus the PI controller has the same values as the control system 1, and for the control loop of the synchronous machine speed, the PI controller has $k_p = 9.5$ and $k_i = 0.005$.

The system based in the flywheel has two constraints in the discharge mode:

Minimum voltage level of the $V_{DC-link}$ voltage of the direct current bus, which is calculated by means of Equation 13 [10]. For this work, the minimum voltage is $V_{dc_minimum} = 639V$.

Discharge depth of the flywheels. This is calculated as the 75 % of its stored energy, which for this case is $w_{r_minimum} = 27rad/s$.

$$V_{DC_minimum} = \frac{2\sqrt{2}V_{f-n(rms)}}{D_q} \quad (13)$$

If the system based on flywheels is below the constraints in discharge mode, the reference current is fixed to a value of 0, so that it does not supply nor absorb power during the occurrence of a voltage sags at the CCP.

3. Results and Discussion

3.1. Performance of the control system

In order to verify the performance of the system based on flywheel, the limits established in section 3 are considered. On that basis, the model of Figure 1 is simulated, without including the system based on flywheel. The resulting voltage level is illustrated in Figure 6.

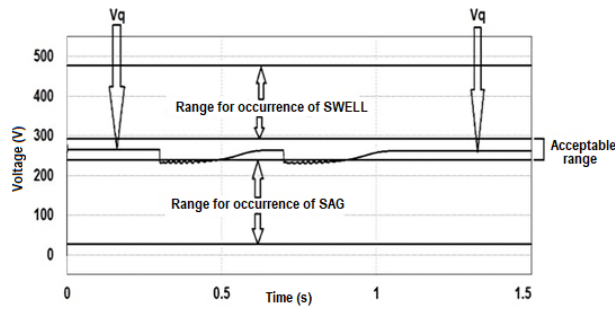


Figure 6. Behavior of the voltage at the CCP at the moment of starting the motors in the distribution network, without the power system based on flywheels.

From Figure 6 it can be seen that before starting the operation of the loads ($t < 0,3$ s) the voltage level at the CCP is 265.5 V, which is between the acceptable margins established in section 3 and with a current of 13 A (Figure 7), due to the charge of 20Ω which is connected.

At the moment when the first electric motor starts ($t \geq 0,3$ s), a sudden and transient decrease in voltage is observed with a value of 231 V (Figure 6), which demands a peak current of 400 A with a duration time of 0.2 s, as indicated in Figure 7. In this condition, the voltage at the CCP is in the range established for the occurrence of a voltage sag.

The time in which the voltage level enters again in the acceptable range is 0.2 s (Figure 6).

Such behavior occurs again in 0.7 s, because the second motor is connected, with the same value of peak current and stabilization time.

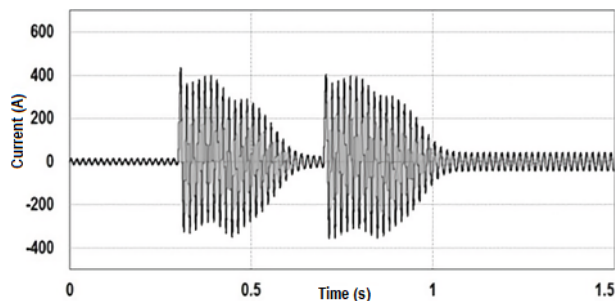


Figure 7. Behavior of the current in phase «A» at the CCP, at the moment of start-up of the electric machine in the distribution network, without the power system based on flywheels.

The connection of the power system based on flywheels is now considered, which supplies energy to mitigate the voltage sags at the CCP, resulting in Figure 8.

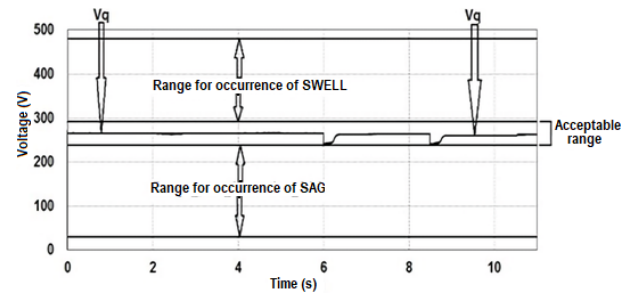


Figure 8. Voltage level by including the power system based on flywheels to mitigate voltage sags at the CCP.

It can be seen in Figure 8 that at the start-up instant of the first motor, which is 6 s, the voltage level is inside the acceptable range established in section 3, with a value of 244 V, compared to the voltage level of Figure 6 it increased 13 V. Similarly, it occurs at 8.5 s when the second motor starts with a voltage level of 244 V at that instant.

It can be seen in Figure 9 the voltage $V_{DC-link}$ and the synchronous machine speed. The following events are observed: before the motors start the voltage $V_{DC-link}$ increases up to a reference value of 900 V, with the associated power converter operating as a rectifier so that the distribution network can absorb power, with its corresponding current loop with negative reference equal to -20 A (Figure 10a).

It is important to remark that in this condition, the current of the system based on flywheel known as I_{filter} is out of phase with the current that circulates through the load (Figure 10a). Similarly, it is observed in Figure 9 that the synchronous machine speed starts to increase up to a reference value of 200 rad/s with the associated power converter operating as an inverter, so that the flywheel absorbs power from the $V_{DC-link}$ voltage source, with its corresponding current loop with positive reference equal to 40 A (Figure 11). In this state the power system based on flywheel is in charging mode.

When the synchronous machine reaches the corresponding reference speed operating as a motor, it consumes a total current of 3.8 A (Figure 11). In this state the power system based on flywheel is in stand-by mode.

At time $t \geq 6$ s of Figure 9 it is observed a sudden decrease in the voltage $V_{DC-link}$ with a value equal to 860 V, which is due to the start of the first motor connected to the CCP, and at this instant the associated power converter operates as inverter to supply power to the distribution network, with the corresponding current loop with positive reference equal to 115 A (Figure 10b). An important aspect is that the current supplied to the network by the system based on flywheel, known as I_{filter} , is in phase with the current that circulates through the load (Figure 10b).

To avoid that the $V_{DC-link}$ decreases sharply, the synchronous machine starts operating as a generator reducing its velocity up to a value of 164.3 rad/s, delivering power by means of the power converter in rectifier mode to the $V_{DC-link}$ voltage source, with the corresponding current loop with negative reference equal to -100 A (Figure 11).

The decrease of the $V_{DC-link}$ voltage and the machine speed are maintained during the start of the

motor, which is of 0.2 s. In this state, the system based on flywheel is in discharge mode.

Once the start time of the motor has passed and when the voltage at the CCP is in the range established in section 3, the $V_{DC-link}$ voltage jointly with the machine speed increase again up to their reference values (Figure 9), and the previously mentioned cycle is repeated again when another voltage sag occurs.

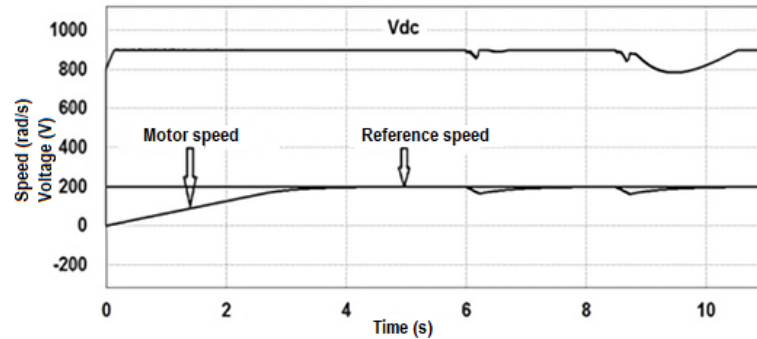


Figure 9. $V_{DC-link}$ voltage and synchronous machine speed.

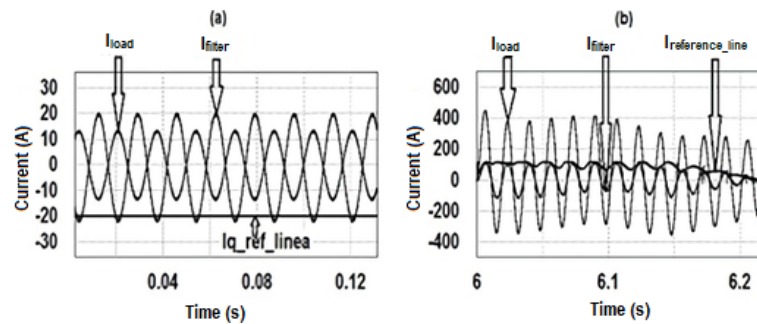


Figure 10. Reference current of the power system based on flywheels: a) charge mode, b) discharge mode.

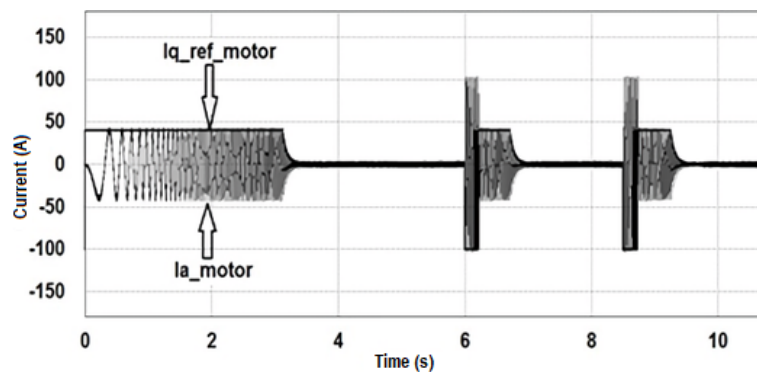


Figure 11. Reference current for the synchronous machine.

Another important aspect is the THD level at the charge, stand-by and discharge moments of the system based on flywheel. After the simulation test, the following results were obtained: 1) regarding the THD of the current that circulates to the load it was obtained 2.4 %, less than the established which is 8 % (standards CONELEC 004/01, NP EN 50160-2010), 2) regarding the THD of the voltage measured at the CCP it was obtained 2.4 %, less than the established in the standard, 3) regarding the THD of the current that circulates to the system based on flywheel it was obtained 3.4 %, less than the established in the standard.

4. Conclusions

The present paper carries out a study about the voltage levels caused by the incorporation to a distribution network of a power system based on flywheels, in the presence of voltage sags caused by the entry of transient loads to the electrical network.

According to the results presented, it can be concluded that the voltage level is regulated in the distribution network, when the system is loaded with the presence of loads in the electrical network.

The system exhibits a response time smaller than milliseconds, thus avoiding the occurrence of voltage sags in the CCP at the moment when important loads connected to the network are started.

Another important aspect is that the power system based on flywheel does not affect the THD levels of the voltage and current at the CCP.

A limitation of this system is that it will not be able to compensate a voltage swell once the nominal load condition is reached, because it will not have additional capacity to absorb the excess power at the CCP, since both the voltage of the direct current bus and the synchronous machine speed already reached their nominal values.

If no actions are taken, the useful life of each of the components of the system will deteriorate, shortening its operating time.

A problem of this system is that, if the voltage level of the direct current bus and the synchronous machine speed are below the minimum allowed values, the system will not be able to supply energy to avoid the occurrence of voltage sags, and if at that instant the control systems behaves incorrectly, the system based on the flywheel will start absorbing power from the network thus entering in the charge mode, involving directly a more severe decrease of the voltage level at the CCP.

To overcome this problem, an auxiliary power supply system must be installed in parallel, which should consist of a control system that jointly monitors: the voltage level of the direct current bus, the synchronous machine speed and the distribution network voltage, since in this way, when the system based on the flywheel and the distribution network are below the allowed values, it starts supplying power to avoid the occurrence of voltage sags at the CCP.

Acknowledgement

The first author thanks to the Secretaría de Educación Superior, Ciencia, Tecnología e Innovación (Senescyt) of the Republic of Ecuador, for the fourth level scholarship.

References

- [1] N. S. Gayathri, N. Senroy, and I. N. Kar, "Smoothing of wind power using flywheel energy storage system," *IET Renewable Power Generation*, vol. 11, no. 3, pp. 289–298, 2017. [Online]. Available: <https://doi.org/10.1049/iet-rpg.2016.0076>
- [2] D. O. Akinyele and R. K. Rayudu, "Review of energy storage technologies for sustainable power networks," *Sustainable Energy Technologies and Assessments*, vol. 8, pp. 74–91, 2014. [Online]. Available: <https://doi.org/10.1016/j.seta.2014.07.004>
- [3] S. Gayathri Nair and N. Senroy, "Power smoothening using multi terminal dc based dfig connection and flywheel energy storage system," in *2016 IEEE 6th International Conference on Power Systems (ICPS)*, 2016, pp. 1–6. [Online]. Available: <https://doi.org/10.1109/ICPES.2016.7584134>
- [4] J. A. Guacaneme, D. Velasco, and C. A. L. Trujillo, "Revisión de las características de sistemas de almacenamiento de energía para aplicaciones en micro redes," *Información tecnológica*, vol. 25, pp. 175–188, 00 2014. [Online]. Available: <https://bit.ly/3bMXPSE>
- [5] D. R. Aitchison, M. Cirrincione, and N. Leijtens, "Design development of a flywheel energy storage system for isolated pacific island communities," in *2016 IEEE International Conference on Advanced Intelligent Mechatronics (AIM)*, 2016, pp. 1628–1633. [Online]. Available: <https://doi.org/10.1109/AIM.2016.7577003>
- [6] J. Itoh, T. Masuda, D. Sato, T. Nagano, T. Suzuki, and N. Yamada, "Development of magnetic assist system in flywheel energy storage system for power load-leveling," in *2016 IEEE International Conference on*

- Renewable Energy Research and Applications (ICRERA)*, 2016, pp. 198–203. [Online]. Available: <https://doi.org/10.1109/ICRERA.2016.7884537>
- [7] X. Zhang and J. Yang, “A robust flywheel energy storage system discharge strategy for wide speed range operation,” *IEEE Transactions on Industrial Electronics*, vol. 64, no. 10, pp. 7862–7873, 2017. [Online]. Available: <https://doi.org/10.1109/TIE.2017.2694348>
- [8] F. Franco Hernández and H. Valdés Carrillo, *Minería artesanal del oro de aluvi3n en Mocoa, Putumayo, Amazonia colombiana*. Universidad Nacional de Colombia, 2005. [Online]. Available: <https://bit.ly/2zTe5uL>
- [9] G. V. Deshpande and S. S. Sankeshwari, “Speed control of induction motors using hybrid pi plus fuzzy controller,” *International Journal of Advances in Engineering & Technology, IJAET*, vol. 6, no. 5, pp. 2253–2261, 2013. [Online]. Available: <https://bit.ly/3dYCspA>
- [10] L. G. González Morales, “Mejora de la eficiencia y de las prestaciones dinámicas en procesadores electrónicos de potencia para pequeños aerogeneradores sincr3nicos operando en r3gimen de velocidad variable,” Ph.D. dissertation, 2011. [Online]. Available: <https://bit.ly/2Tqfksm>
- [11] F. A. Bardemaker, “Modula33o vetorial aplicada a retificadores trifásicos PWM unidireccionais,” Ph.D. dissertation, 2006. [Online]. Available: <https://bit.ly/3e5gsta>
- [12] A. S. de Moraes, F. Lessa Tofoli, and I. Barbi, “Modeling, digital control, and implementation of a three-phase four-wire power converter used as a power redistribution device,” *IEEE Transactions on Industrial Informatics*, vol. 12, no. 3, pp. 1035–1042, 2016. [Online]. Available: <https://doi.org/10.1109/TII.2016.2544248>
- [13] S. M. de Pancorbo, G. Ugalde, J. Poza, and A. Egea, “Comparative study between induction motor and synchronous reluctance motor for electrical railway traction applications,” in *2015 5th International Electric Drives Production Conference (EDPC)*, 2015, pp. 1–5. [Online]. Available: <https://doi.org/10.1109/EDPC.2015.7323219>
- [14] M. Bhardwaj, *Sensored Field Oriented Control of 3-Phase Permanent Magnet Synchronous Motors*. Texas Instruments, 2013. [Online]. Available: <https://bit.ly/3gahvKc>
- [15] S. Talebi Rafsanjan, “Advanced high-speed flywheel energy storage systems for pulsed power application.” Ph.D. dissertation, 2008. [Online]. Available: <https://bit.ly/3cPPO7j>